Spatial Sharpening of Thematic Mapper Multispectral Images with a Higher Resolution Panchromatic Band Image

By George Lemeshewsky

Open File Report 96-302

U.S. Department of the Interior
U.S. Geological Survey
National Mapping Division

SPATIAL SHARPENING OF THEMATIC MAPPER MULTISPECTRAL IMAGES WITH A HIGHER RESOLUTION PANCHROMATIC BAND IMAGE

George Lemeshewsky
U.S. Geological Survey
521 National Center
Reston, VA 22092
Open-File Report 96-302

ABSTRACT

A method for spatial resolution enhancement, or sharpening of three bands of a Landsat thematic mapper (TM) multispectral image by a higher resolution SPOT panchromatic (pan) image, is described. Visible band TM images having positive correlation with the geometrically coregistered pan image are sharpened with a reported multiresolution sharpening technique. Application of neural network estimation technique is described to improve sharpening of near-infrared bands specifically when there are reverse contrast patterns at respective edge boundaries of the pan and TM images. Unless corrections are made for reverse patterns there will be degraded sharpening. Thus multilayer feedforward neural networks are trained to adaptively estimate, at multiple resolutions, pan edge patterns that have the same contrast as the TM edge patterns. Using this estimated data with a reported multiresolution sharpening technique gives spatial resolution enhancement. Image examples illustrate opposite contrast edges of pan and near-infrared TM bands. Other examples show improved sharpening when neural network modified edge information is combined with the multiresolution sharpening methods.

Any use of trade, product, or firm names is for descriptive purposes only and does not imply endorsement by the U.S. Government.

I. INTRODUCTION

There are many reported techniques for sharpening or enhancing the resolution of a multispectral image by integrating spatial information from a higher resolution panchromatic image. This report describes a technique developed specifically to improve sharpening when opposite contrast patterns occur at edge boundaries of panchromatic (pan) and multispectral (MS) images. In this case, a reported multiresolution technique that transfers edge information to the lower resolution image is used for sharpening, but edge data are first modified to correct for opposite contrast conditions. Without this modification, there is degraded sharpening. The sharpening process is described for three thematic mapper (TM) 30-m bands and a SPOT 10-m pan image.

II. BACKGROUND

Schowengerdt (1980) reported early experiments in multispectral sharpening by the addition of edge information obtained by high-pass filtering of a higher resolution image and described problems that occur when contrast reversals exist at edge boundaries of MS images. Roughly, the high-pass filtered image with zero average value has localized positive-negative transitions at contrast boundaries. Opposite contrast boundaries have a reversed positive-negative transition, hence reversed or opposite signs.

The sign of multispectral edges can change from band to band; for example at soil/vegetation boundaries. Schowengerdt (1980) described an adaptive procedure that changed edge signs, depending upon band-to-band contrast reversals and a mechanism for detecting such boundaries: the sign of the product of high-pass derived edges is negative for opposite contrast edges patterns. Without the sign correction step, there is degraded sharpening because the edges subtract, instead of add, to the edge boundary.

Another sharpening technique, described by Tom, Carlotto, and Scholten (1985) makes use of the local correlation between TM multispectral band images at contrast boundaries. They developed a least-squares (LS) modeling approach to optimally model the 120-m resolution infrared-band (IR) image from its local correlation to the remaining six MS bands. To sharpen IR data, the remaining six 30-m TM bands were first filtered to give 120-m spatial resolution. At each sample location of this reduced resolution imagery, a spatially localized (5-by 5-sample window) LS estimator for the IR data was computed from the remaining TM bands. An optimal prediction of the IR image at higher spatial resolution (30 m) was computed from the LS model and remaining 30-m images. This IR image was high-pass filtered and the resulting edges (with same sign) added to the original IR image to produce sharpened IR data.

A method for sharpening by a factor of two, using multiresolution image analysis and neural network (NN) prediction techniques was described by Iverson and Lersch (1994) for a SPOT pan (resampled to 15 m) and 30-m TM image. Their sharpening was described for Laplacian (L) image pyramids. Basically, the images were decomposed into multiresolution, L pyramid edge detail images at sample distances of 30 and 15 m. At reduced resolution, where there was high local spatial correlation between the 30-m pan and TM edge images, a NN was trained to predict

TM edge samples given a small neighborhood pan edge samples. At the higher resolution level, (15 m) of the *L* image pyramid, the previously trained NN predicted a higher resolution TM edge image given the 15-m pan edge image. Finally, the sharpened image was reconstructed from the TM image pyramid and predicted TM edge image.

Multiresolution *L* image pyramid techniques for sharpening images with different degrees of blur was described by Ogden and others (1985). A sharpened image is produced by retaining or replacing individual edge samples of the lower resolution image with those from the higher resolution image based on a maximum selection rule (MR) and then reconstructing the lower resolution image.

Burt and Kolczynski (1993) observe that for opposite contrast edge patterns, maximum selection can be unstable and result in pattern cancellations. They describe a method to identify opposite contrast edge features based on a local measure of correlation. Depending on the correlation value, which ranges from -1 to 1 for opposite to same contrast patterns, edge information is either combined by weighted average, or for extreme values combined by selection.

This report describes an improvement to multiresolution sharpening by maximum replacement of edge samples when there are opposite contrast patterns. Basically, NN estimation techniques were developed that modify the higher resolution edge information so that the maximum selection (for sharpening) is between same sign edge patterns.

III. OVERALL APPROACH

One way to improve the stability of maximum selection of opposite sign edges is to reverse the edge signs, based on local contrast patterns. This technique shares similarities with the previously described predictive sharpening (Iverson and Lersch, 1994), which used multiresolution techniques and NN's (trained at lower resolutions) to predict higher resolution MS edge images. Common to both are NN's trained with data from Laplacian pyramid images.

However, in this application sharpening is the result of combining (by MR) given edge images after sign modification by NN's, instead of predicting higher resolution edge images. Inputs to the NN are the pan edge image and a mask image calculated from pan and TM edge images. The function of the mask image is similar to the previously mentioned product image (Schowengerdt, 1980) for locating opposite sign edges. However, there are major differences: (1) the mask image is derived from *L* pyramid images, (2) a different product-like calculation was used, and (3) adaptive gray-scale normalization of the *L* edge images was used.

Toet and others (1989) described image fusion with ratio image pyramids (similar to *L* pyramids) and a maximum selection rule to fuse visible and near-infrared images. This gives sharpening when image pairs only differ in blur, and contrast image fusion when spatial detail differ, because the 'best' (that is, larger amplitude) edge information from either image is selected, sample by sample. As described later, NN's were trained specifically to preserve both sharpening and fusion properties inherent with maximum selection of edge samples.

IV. MULTIRESOLUTION SHARPENING

The following is a brief overview of Gaussian (G) and Laplacian (L) image pyramids; see Ogden and others (1985) and Burt and Adelson (1983) for additional details. Figure 1 shows G and L image pyramids for a SPOT pan image; the numeric subscript denotes the pyramid level.

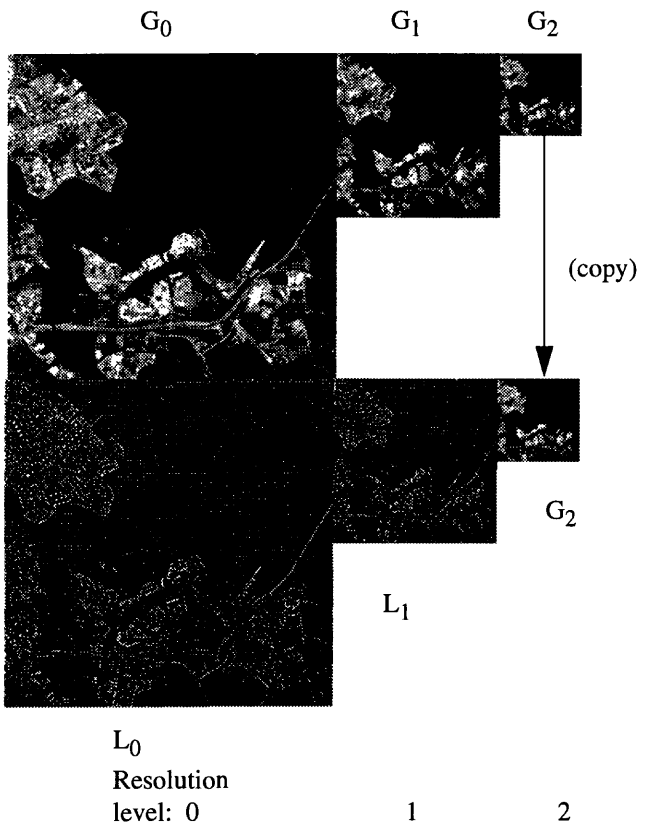

Figure 1. Example of Gaussian (G) and Laplacian (L) multiresolution image pyramids for SPOT panchromatic (pan) data.

G_0 , G_1 , G_2, are a three resolution level (levels 0, 1, 2) G image pyramid for the full resolution, 10-m ground sample distance SPOT (SPOT, 1988) pan image, G_0. Images L_0 and L_1 are pyramid derived L edge data from G_0 and G, respectively. To ensure positive values for display, a gray-level value of 128 was added to the L images. The original pan image, G_0 can be reconstructed exactly from L_0, L_1, and G_2; that is, the Laplacian-Gaussian pyramid decomposition of G_0.

The L images contain edge features derived at multiple resolutions. They are comparable to the results of band-pass-like filtering the G images with nondirectional filters. The images were computed as follows. Starting with the original image at full resolution level 0 (that is G_0), image G_1

is the result of low-pass filtering G_0 followed by subsampling by a factor of two. This process is called reduce, (*RE*). Each *G* image is reduced in size, in each dimension, relative to original image G_0 by 2^{-k}, where *k* is the image pyramid level.

Image L_0 at level 0 is generated by first up-sampling (by a factor of two) image G_1 followed by interpolation; subtracting this result from G_0 gives L_0. Up-sampling followed by interpolation is called expand, (*EX*). Similarly L_1 is computed by applying *RE* and *EX* to G_1 followed by subtraction from G_1.

Low-pass filtering and interpolation was done by convolution with Gaussian-like filters. This study used the separable kernel (1, 4, 6, 4, 1) (Burt, 1985). *G* and *L* image pyramid generation is as follows (Ogden and others, 1985):

$$G_1 = RE[\, G_0 \,] \tag{1}$$

$$L_0 = G_0 - EX[\, G_1 \,] \tag{2}$$

$$G_2 = RE[\, G_1 \,] \tag{3}$$

$$L_1 = G_1 - EX[\, G_2] = G_1 - EX[\, RE[\, G_1 \,]]. \tag{4}$$

Rearranging equation 2 shows that G_0 can be reconstructed exactly from L_0 and G_1:

$$G_0 = L_0 + EX[\, G_1]. \tag{5}$$

Also from equations 4 and 5, G_0 can be reconstructed exactly from

$$G_0 = L_0 + EX[\, L_1 + EX[\, G_2 \,]]. \tag{6}$$

The sharpening of one image with another of higher resolution was reported by Ogden and others (1985) using *L* image pyramids and a maximum selection rule for replacing their samples. For use in later discussion, this rule is described for TM and pan images and three level pyramid decomposition as in equation (6).

Given registered TM and higher resolution pan images, each decomposed into Laplacian pyramid images, the maximum selection rule (Ogden and others, 1985) to get the new edge image L'_{TM} is

if $| L_P(x, y) | > | L_{TM}(x, y) |$ then

$$L'_{TM}(x, y) = L_P(x, y)$$

else

$$L'_{TM}(x, y) = L_{TM}(x, y) \tag{7}$$

end if

where L_P and L_{TM} are *L* pyramid images. Reconstructing the TM image from L'_{TM} and highest pyramid level $G_{2,TM}$ by equation 6 produces the sharpened image. Note that in areas where there are no pan edges (that is, L_P is zero), the TM image will be recovered exactly. Similarly, if there are no TM edges, pan edge details will be transferred and integrated into the reconstructed image. Figure 1 showed the reversible, without reconstruction error *L, G* pyramid image decomposition

for three resolution levels (k=0, 1, 2).

This study developed NN techniques that modify the sign of pan edges, (L_P), prior to the max selection of equation 7.

V. NEURAL NETWORK PROCESSING

The following is a brief description of a multilayer, feedforward (MLFF) neural network. For further information on NN's see Rumelhart and others (1986).

NN or artificial NN is any computing architecture that consists of massively parallel interconnection of simple "neural" processors (Lau and Widrow, 1990). Often (as in this study) multilayer NN's are computer simulations of interconnected "neural" processors or artificial neurons modeled as the net sum of the input signal to the neuron -times- interconnection weight, followed by a nonlinear mapping of net sum to produce the neuron output. Net sum also includes a bias value input; it is equal to the bias weight times its corresponding +1.0 input signal. The nonlinear transfer function in this application was the common sigmoid: f(net sum) = $1 / (1 + e^{-(\text{net sum})})$.

Starting with the inputs, a MLFF NN consists of consecutive layers of neurons, and at each layer, each neuron output is connected to all inputs of the next layer. A simple, one hidden layer MLFF NN (that is, two layer network, Hertz and others, 1991) is shown in figure 2. The NN's for this study had 50 inputs, 1 hidden layer of 5 neurons, and 1 output neuron, denoted (50:5:1).

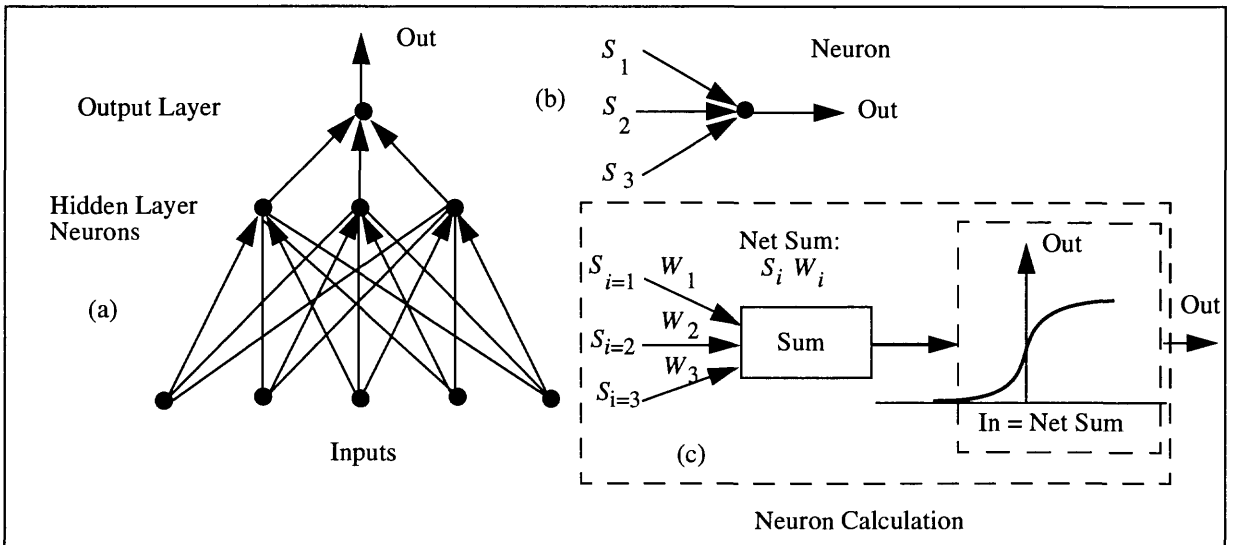

Figure 2. Simple one hidden layer, feedforward neural network (NN).

(a) Shows a multilayer, feedforward, fully connected NN with three 'neurons' or processing elements, (b) in the hidden layer. (c) Shows the calculation performed by each processing element (b): the net sum of input, S_i times connection weight, w_i, followed by a nonlinear mapping of net sum to neuron output.

VI. NEURAL NETWORK TRAINING

The NN's were trained with simulated edge data to implement a mapping of input edge patterns to the output: pan edge sample with sign modification. This mapping is achieved by training, or adjusting the NN weights, that is, presenting the NN with numerous and repeated examples of input-to-desired output and then adjusting the network weights, as a function of the error between desired and actual output such that the NN output approximates the desired output. Because the hidden layer(s) have no direct connection to the output, the output error is propagated back to the hidden layer. Backpropagation training by the generalized rule with momentum (Rumelhart and others, 1986) was used.

NN inputs for one output sample were the 5-by 5-neighbor samples from pan edge and mask images, respectively. Thus the output is estimated from a small local area of edge samples instead of a single location.

To make a TM-like image for training (denoted TM_S) that simulates positive or reverse contrast conditions, or both, of pan-TM images, a SPOT pan image was simply low-pass filtered (Gaussian filter) until it visually matched the TM visible band 3 image and, as required, its gray scale reversed.

Mask image, m(x, y) was calculated as:

$$m(x, y) = \underset{n, TM}{\text{sign}}[L(x, y)] \; [\, | \underset{n, pan}{L}(x, y) | \; | \underset{n, TM}{L}(x, y) | \,]^{1/2} \tag{8}$$

with 1/2 power to reduce the numerical range. $L_{n, TM}$, $L_{n, pan}$ are normalized images with approximately equal amplitude edges. They were computed by dividing each sample, $L(x, y)$, by the average of the absolute values of the sample and its 3-by-3 neighbors. The sign of m(x, y) is either the same or opposite to the pan edge sign, depending on whether L_{pan} and L_{TM} have same or opposite contrast edge patterns.

The overall sharpening process for the TM near-IR band 4 image sharpened by SPOT pan image, and including NN correction for opposite contrast edge patterns, is shown in figure 3 for a two Laplacian level pyramid. The third level has the reduced level Gaussian image (see equation 6).

The NN training data, used to establish the mapping of input edge patterns to output edge sample, were derived from several combinations of the pan image and a simulated (blurred, gray-scale reversed pan) MS image, denoted TM_S.

Table 1 illustrates the objectives of NN training for the following conditions: (a) sign modification (1,2); (b) pan edges when no TM_S edges (3); and (c) TM_S edges and no pan edges (4). Note that NN inputs are the pan and mask images.

The right column of table 1 shows the result of maximum selection of TM edge samples when applied to NN output and TM samples. To preserve the fusion of pan edge information, NN output for training condition 3 was defined to be pan edge samples. That is, NN's were trained to produce pan edge patterns when there are no TM edge patterns. Small random number values were used in place of mask image values of zero to better simulate noise in the edge data.

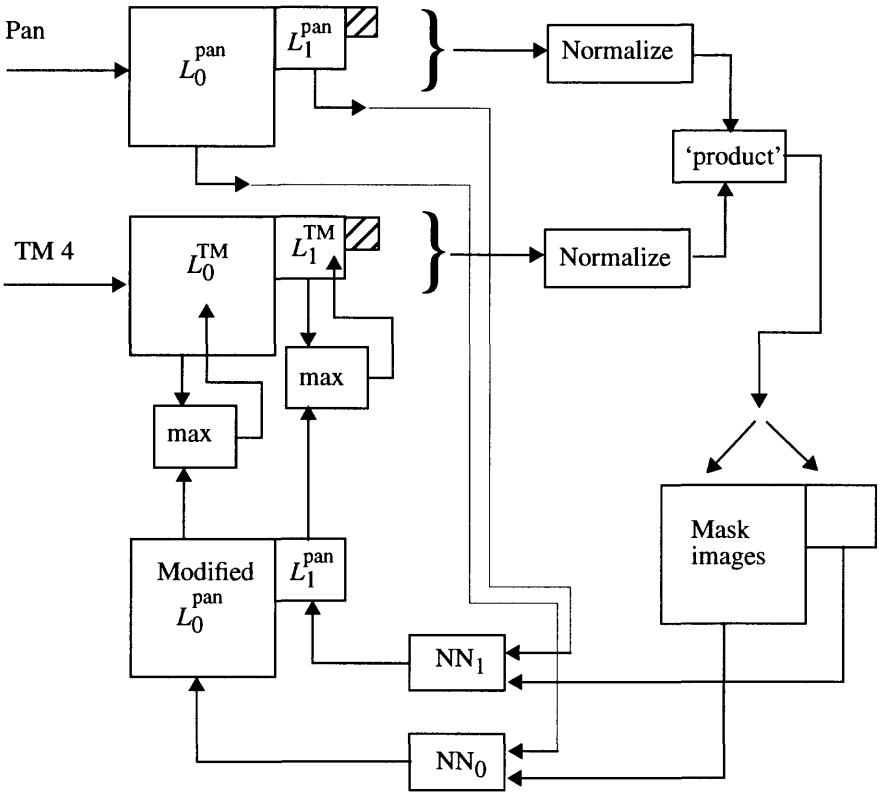

Figure 3. Multiresolution sharpening of a TM band image with neural network correction for opposite contrast patterns.

This shows the overall sharpening process after the pan and XS images are decomposed to multiresolution, Laplacian pyramid images. Neural networks NN_0, NN_1, whose inputs are 5 by 5 samples from each pan and edge mask image, adaptively modify (reverse sign) the pan edge sample when pan-TM images have opposite contrast patterns.

TM edge pattern samples are replaced using a maximum (max) selection and replacement rule applied to TM and modified pan edge data. Sharpened TM results from reconstructing the TM image from its replaced edge samples.

For training condition 4, maximum selection preserves the TM image details. Because NN inputs are pan and mask edge images, training data for these conditions occur where there are no pan edges. Data for conditions 1 and 4 were collected from pan image in areas that included edge boundaries and contrast regions

A NN was trained for each L image level (0,1). Because of their generalization property (similar inputs produce similar outputs), the trained NN's function as estimators for the remaining image,

or other similar images. That is, generalization allows the NN to approximate the correct output when given input samples similar to, but not identical to training set samples (Wasserman, 1993). Separate training and test data sets were from adjacent areas of the *L* edge images. .

Table 1: Network Training Conditions

Training condition	Edges present		TM_S-pan contrast patterns	Mask image	Neural Network Output	Result of maximum replacement
	pan	TM				
1	yes	yes	same	pan$*TM_S$	pan edge	sharpened
2	yes	yes	opposite	- pan$*TM_S$	- pan edge	sharpened
3	yes	no	pan only	zero[1]	pan edge	fusion: pan
4	no	yes	TM only	zero	zero	fusion: TM
NN inputs are the pan and mask images. Zero[1] = small random number values.						

To obtain a small NN, because fewer parameters (that is, number of weights or neurons, or both) improve generalization (Hertz and others, 1991), training started with a larger NN (50:10:1) and reduced the number of hidden layer neurons. Thus a 5 hidden layer NN (50:5:1) was picked because both 5 and 10 neuron hidden layer NN had comparable performance to test set data. This is a relatively simple NN configuration; no other NN sizes were tested.

Next, 2 untrained 50:5:1 neuron networks were trained in increments of about 1(or 3) presentations of the training file. Learning rate and momentum were, respectively: (a) output layer, 0.0750, 0.0075 and (b) hidden layer, 0.1500, 0.0150 . Weight updates were after each sample presentation (NeuralWare, 1993).

Network performance (that is, RMS error) to the test data was computed after each incremental training cycle to give a measure of generalization. Both NN's (level 0, 1) had, for incremental training, a local minimum error to the test data; they were retained for this study. Test error increased and then decreased with further training; this may be because of overtraining.

It is likely that the NN's trained quickly because of many redundant training samples. Network performance to training and test data are summarized in tables 2 and 3; the RMS error is for the NN output range of 0 to 1. The fact that test set error is less than training set error is possibly because of the test file containing many input-output patterns that have low RMS error. The arrow indicates NN's for this study.

Table 2: Neural Network, level 0 performance versus training; 18,432 training and test samples.

NN no.	Cumul. no. of samples, thousands	RMS training error,	RMS test error
1	20	0.0589	0.0513
2 ←	40	0.0579	0.0504
3	60	0.0578	0.0509
4	80	0.0573	0.0509
5	100	0.0567	0.0500

Table 3: Neural Network, level 1 performance versus training; 8064 training and test samples.

NN no.	Cumul. no. of samples, thousands	RMS training error	RMS test error
1	25	0.0441	0.0395
2 ←	50	0.0435	0.0386
3	75	0.0435	0.0388
4	100	0.0430	0.0387

VII. TEST RESULTS

The mask images of figure 4, which illustrate opposite contrast edge patterns, were computed from the product of pan and simulated or actual TM Laplacian level 0 edge images, per equation 8. Mask images are for (a) pan and simulated same contrast TM, (b) pan and simulated opposite contrast TM, and (c) pan and actual TM near-IR band 4 image. A comparison of image 4(c) with 4(b) shows, for example, that there are opposite contrast patterns at the shoreline and highway-vegetation boundaries. Figure 4 includes the SPOT (SPOT, 1988) pan 4 (e) and TM band 4 (d) images.

Figure 5 compares TM near-IR band 4 sharpening with (fig. 5(a)) and without (fig. 5(b)) the NN edge modification/correction for opposite contrast conditions. For the two methods, maximum selection was applied to either pan edge data after its modification by the NN processing to correct for opposite contrast patterns, or unchanged pan edge data.

Sharpening improvements due to NN processing are as follows. Mask image (fig. 4(c)) indicates the location (that is light-to-dark transitions) of sharpened contrast boundaries of figure 5(a), because the mask was derived from the product of pan and TM edge patterns. Thus a comparison between mask (fig. 4(c)), raw TM band-4 (fig. 4(d)), and the NN sharpened TM image (fig. 5(a)) shows where many of the larger contrast boundaries have been sharpened. One example of sharpening with correction for reverse contrast patterns can be seen by comparing (figs. 4(c), 5(a), and 5(b)) the long, narrow feature, that is located parallel to the shore line, and to the upper left of the group of 4-by-3 circular features. This feature is dark (correct) in the NN sharpened image figure 5(a), but light (incorrect) for the maximum selection sharpening of figure (5)b.

Note in figure 5(b) that the result of maximum sharpening is roughly the superposition of edge feature details from the pan image, without compensation for opposite contrast boundaries. Also, the shore line is not as 'sharp' as that of figure 5(a), a result of maximum selection between opposite contrast edge patterns. The 'blocky' appearance of figure 5(a) is possibly related to the mask image, one of the NN inputs of figure 4(c) and is the subject of further study.

Because the spectral response of TM visible bands 3 or 2 is within the SPOT panchromatic band (Richards, 1993), it was assumed that these TM-pan bands have only same contrast edges. Thus bands 3 and 2 were sharpened by maximum selection, without correction for contrast conditions. Also, to improve coregistration of their edge boundaries, the sharpening was performed in the lightness, hue, and saturation domain: (1) TM bands 2, 3, 3 (as red, green, blue) were transformed to lightness, hue, and saturation, (2) the lightness image sharpened, and (3) the sharpened lightness with original hue and saturation images were then transformed to red, green, blue to give sharpened TM2, TM3, TM3. A simpler process is the subject of further study.

Figure 6 shows color images of TM bands 4 (red), 3 (green), and 2 (blue) before and after sharpening. The sharpened image, figure 6(a) is the same figure 5(a),(c),(e); and band 4 included the NN correction for opposite contrast.

VIII. CONCLUSION

Neural networks trained to modify edge features were applied to a reported multiresolution image sharpening process to improve sharpening when there are opposite contrast edge patterns. For sharpening, edge samples of the lower resolution image are replaced with those from a higher resolution image by way of a reported maximum replacement rule. To improve sharpening and prevent pattern cancellations, a NN technique for preprocessing edge samples was developed; it ensures that the maximum rule is applied to same sign edge samples. Thus NN's modify (reverse sign) the higher resolution edge samples depending on local edge patterns of the two images. Also, NN's were trained to transfer edge pattern information from the higher to lower resolution image when the latter had no edge information. Thus, the combined image includes edge information from either image. For the NN preprocessing technique, preliminary results indicate that sharpening of reverse contrast edges is improved. Although these results are promising, further study to improve this technique is needed.

REFERENCES

Burt, P.J., and Kolczynski, R., 1993, Enhanced image capture through fusion: Proc. of the Fourth International Conf. on Computer Vision, IEEE Computer Society, 1993, p. 173-182.

Burt, P.J., and Adelson, E.H., 1983, The Laplacian pyramid as a compact image code: IEEE Trans. on Communications, v. 31, no. 4, p. 532-540.

Hertz, J., Krogh, A. and Palmer, R., 1991, Multi-layer Networks, chapt. 6 *in* Introduction to the Theory of Neural Computation: Addison-Wesley, p. 115-162.

Iverson, A.E., and Lersch, J.R., 1994, Adaptive image sharpening using multiresolution representations: Proceedings SPIE, v. 2231, p. 72-83.

Lau, C.G., and Widrow, B., 1990, Scanning the Issue - Neural Networks, I: Theory and Modeling: Proceedings of the IEEE, v. 17, no. 9, p. 1411-1413.

NeuralWare, Inc., 1993, Neural Computing. Pittsburgh, PA, NeuralWare.

Ogden, J.M., Adelson, E.H. and Bergen, J.R., and Burt, P.J., 1985, Pyramid based computer graphics: RCA Engineer, v. 30, no. 5, p. 4-15.

Richards, J.A., 1993, Sources and Characteristics of Remote Sensing Image Data, chapt. 1 *in* Remote Sensing Digital Image Analysis: Springer-Verlag, Berlin, p. 1-37.

Rumelhart, D.E., Hinton, G.E., and Williams, R.J., 1986, Learning Internal Representations by Error Propagation, chap. 8 *in* Parallel Distributed Processing 1: Foundations, D.E. Rumelhart and J.L McClelland, MIT Press, Cambridge, MA, p. 318-362.

Schowengerdt, R.A., 1980, Reconstruction of multispectral image data using spatial frequency content: Photogrammetric Engineering and Remote Sensing, v. 46, no. 10, p.1325-1334.

SPOT Image Corporation, 1988: SPOT Image Corp., Reston, VA.

Toet, A., vanRuyven, L.J., and Valeton, J.M., 1989, Merging thermal and visual images by a contrast pyramid: Optical Engineering, v. 28, no. 7, p. 789-792.

Tom, V.T., Carlotto, M.J., and Scholten, D.K., 1985, Spatial sharpening of Thematic Mapper data using a multiband approach: Optical Engineering, v. 24, no. 6, p. 1026-1029.

Wasserman, P.D., 1993, Neural engineering, chap. 11 *in* Advanced methods in neural computing: NewYork, VanNostrand-Reinhold, p. 214-244.

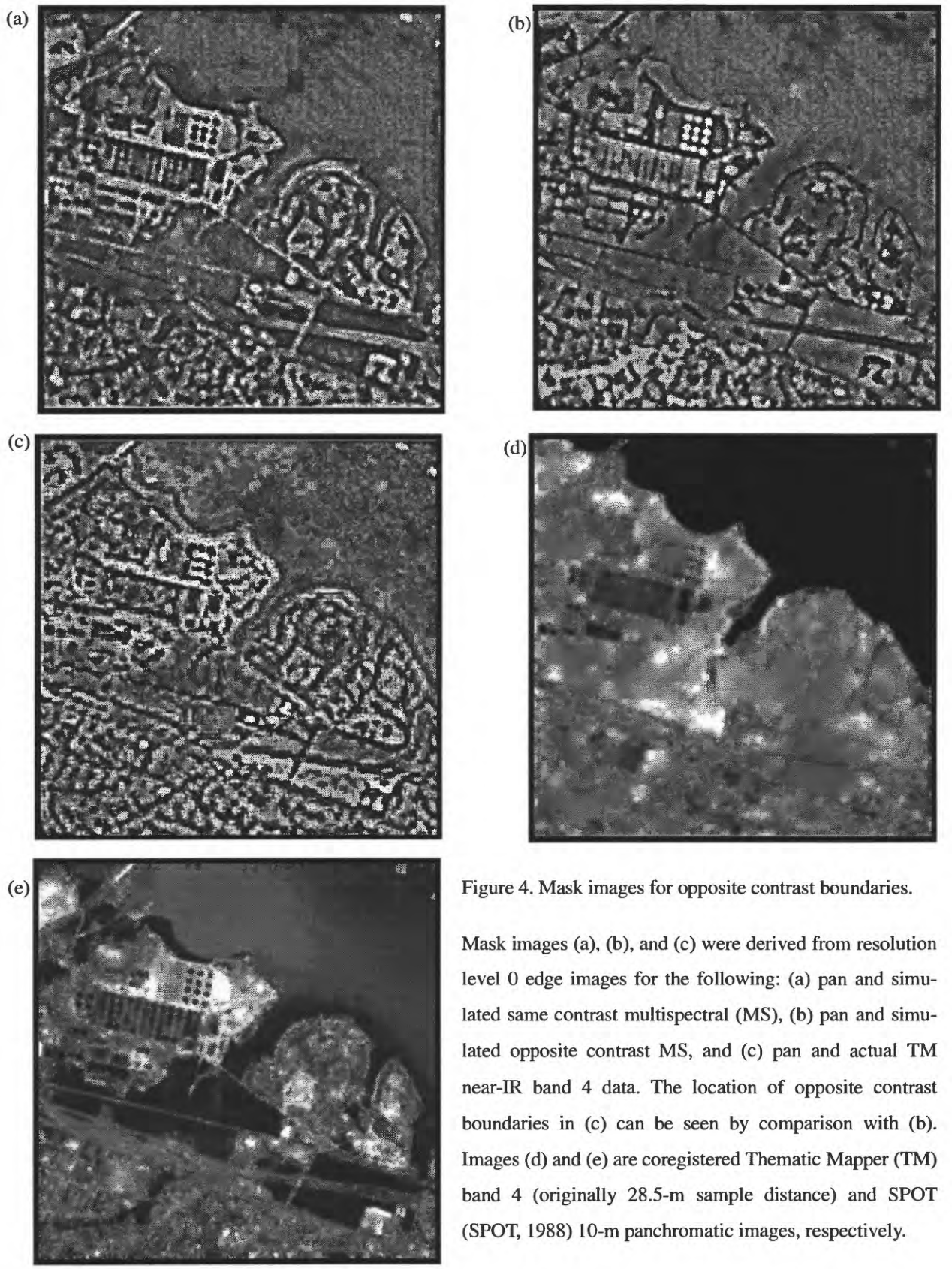

Figure 4. Mask images for opposite contrast boundaries.

Mask images (a), (b), and (c) were derived from resolution level 0 edge images for the following: (a) pan and simulated same contrast multispectral (MS), (b) pan and simulated opposite contrast MS, and (c) pan and actual TM near-IR band 4 data. The location of opposite contrast boundaries in (c) can be seen by comparison with (b). Images (d) and (e) are coregistered Thematic Mapper (TM) band 4 (originally 28.5-m sample distance) and SPOT (SPOT, 1988) 10-m panchromatic images, respectively.

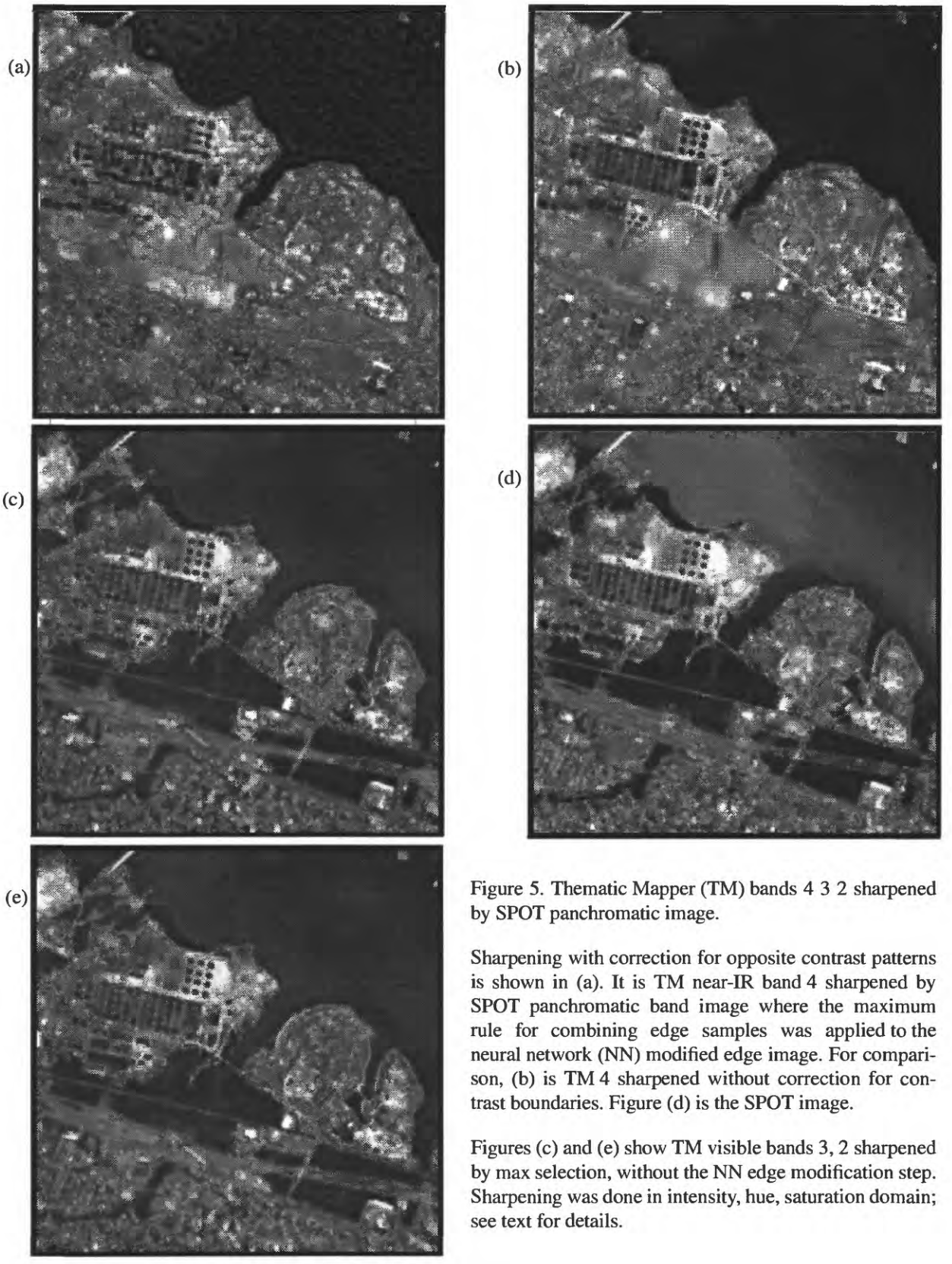

Figure 5. Thematic Mapper (TM) bands 4 3 2 sharpened by SPOT panchromatic image.

Sharpening with correction for opposite contrast patterns is shown in (a). It is TM near-IR band 4 sharpened by SPOT panchromatic band image where the maximum rule for combining edge samples was applied to the neural network (NN) modified edge image. For comparison, (b) is TM 4 sharpened without correction for contrast boundaries. Figure (d) is the SPOT image.

Figures (c) and (e) show TM visible bands 3, 2 sharpened by max selection, without the NN edge modification step. Sharpening was done in intensity, hue, saturation domain; see text for details.

(a)

(b)

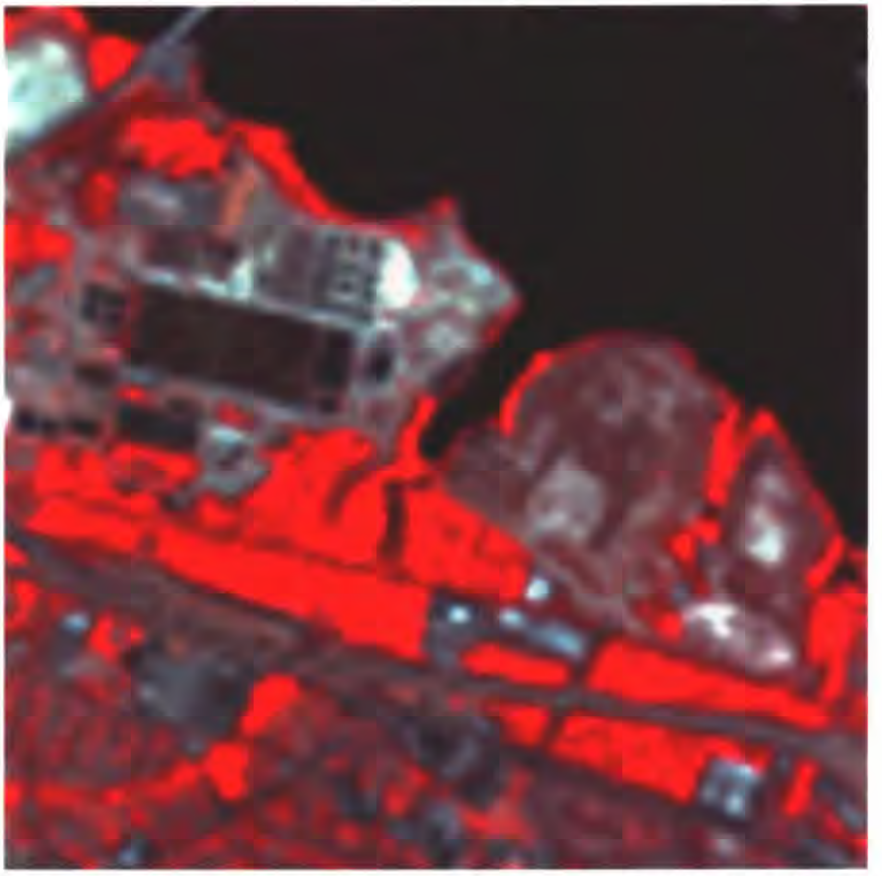

Figure 6. Color examples of sharpened and unsharpened TM band 4 3 2 images.

TM bands are displayed as 4 (red) 3 (green) 2 (blue). Image (a) is the sharpened TM band 4 3 2 image, with NN edge correction process applied to band 4. This is the color display of figure 6 (a,b,c). Image (b) is the unsharpened TM image.